

# Charge-coupled device area detector for low energy electrons

Miroslav Horáček<sup>a)</sup>

*Institute of Scientific Instruments, Academy of Sciences of the Czech Republic, Královopolská 147,  
CZ-61264 Brno, Czech Republic*

(Received 27 December 2002; accepted 28 April 2003)

A fast position-sensitive detector was designed for the angle- and energy-selective detection of signal electrons in the scanning low energy electron microscope (SLEEM), based on a thinned back-side directly electron-bombarded charged-coupled device (CCD) sensor (EBCCD). The principle of the SLEEM operation and the motivation for the development of the detector are explained. The electronics of the detector is described as well as the methods used for the measurement of the electron-bombarded gain and of the dark signal. The EBCCD gain of 565 for electron energy 5 keV and dynamic range 59 dB for short integration time up to 10 ms at room temperature were obtained. The energy dependence of EBCCD gain and the detection efficiency are presented for electron energy between 2 and 5 keV, and the integration time dependence of the output signals under dark conditions is given for integration time from 1 to 500 ms. © 2003 American Institute of Physics. [DOI: 10.1063/1.1583863]

## I. INTRODUCTION

The progress in low energy electron microscopy includes the enhancement of the surface sensitivity of the information as well as the reduction of the local charging of low conductivity specimens. The range of very low energy electrons with energies below 50 eV is particularly interesting. Micrographs in this mode bring different types of contrast due to the wave nature of the electron.<sup>1</sup> The wave-optical phenomena appear in the backscattered electron signal only when the electron wavelength becomes comparable with interatomic distance, i.e., in the range of  $10^0$ – $10^1$  eV. Typical for interaction of very slow electrons with crystalline surface or thin multilayer is an anisotropic angular distribution exhibiting maxima and minima. In the scanning electron microscope (SEM) the diffraction pattern is formed in the back-focal plane, and it can be directed toward the area detector and recorded separately for every image pixel.

The charge-coupled device (CCD) area detector for low energy electrons, described in this article, was designed for the detection of angular distribution of signal electrons in the scanning low energy electron microscope (SLEEM). The goal was to detect the emitted low energy electrons below 5 keV, to acquire the angular distribution of the emission, and to record for each pixel one full pattern of the angular distribution within a few milliseconds.

## II. ACQUISITION OF MULTIDIMENSIONAL IMAGE IN SLEEM

In the SEM a two-dimensional image of the specimen surface is usually formed pixel by pixel in topographical or material contrast mode, depending on the type of detector used. The conventional detectors work as integral detectors, i.e., they collect all signal electrons incident on them as one data item. All information hidden in the angular or energy

distribution of the emission is then lost. Acquisition of the energy spectrum requires us to insert an energy filter in front of the specimen and to extend the dwell time for every pixel so that the energy spectrum or its selected part can be recorded. Significant progress was recently made by a parallel recording electron spectrometer, equipped with a one-dimensional (1D) line semiconductor detector, enabling one to acquire up to 1000 energy channels at once.<sup>2</sup> The angular distribution of the emission, projected into a plane above the specimen surface, cannot be acquired point by point by a movable single channel detector so that a multichannel 2D detector is required.

Modern computer controlled SEMs are fast enough in all control and data acquisition activities so that a great majority of their operation time is active and the time consumption is proportional to the signal-to-noise ratio (SNR) in the image. When increasing the image dimensionality from 2 to 4, i.e., when for every image pixel a 2D matrix of data points is recorded with a moderate SNR, the acquisition time extends enormously and becomes critical. For the scanning matrix “ $m$  by  $n$ ” of  $512 \times 512$  pixels and maximum affordable time 10 min for one SEM frame we get 2.3 ms for the acquisition of the angular distribution at each specimen point. The total time of 10 min was fixed as a maximum reasonable time from the point of view of operating efficiency and long term stability of the microscope equipped with a multichannel 2D detector.

The proposed detector was designed for a SLEEM arrangement shown in Fig. 1.<sup>3</sup> The column works with the primary beam of several keV, decelerated close to the specimen surface to a desired very low energy in the cathode lens. The combination of the cathode lens with focusing magnetic or electrostatic lens (so-called immersion objective lens) ensures significantly lower aberrations at very low energies than the focusing lens alone.<sup>4,5</sup>

The signal electrons passing backward through the immersion objective lens are accelerated by the cathode lens

<sup>a)</sup>Electronic mail: mih@isibmo.cz

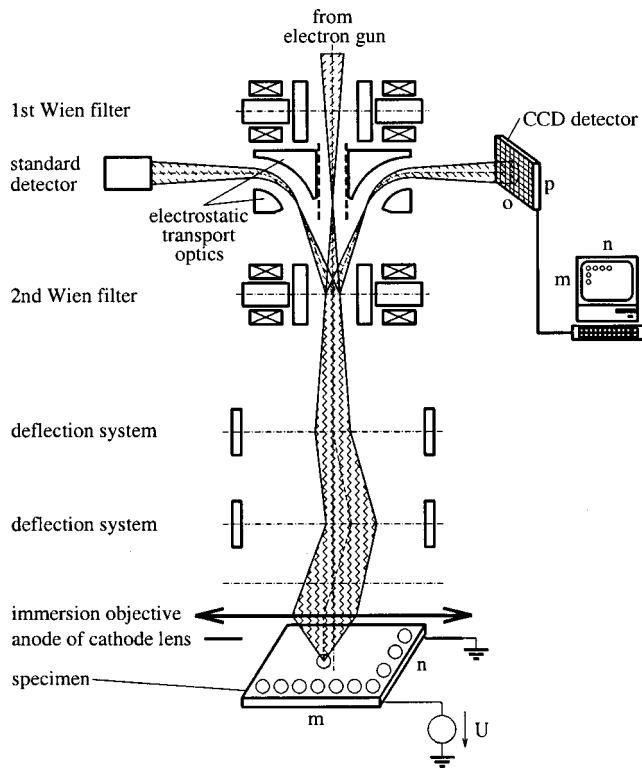


FIG. 1. SLEEM with EBCCD detector.

and collimated toward the optical axis so that their angular distribution is preserved. Behind the objective lens the diffraction spots are focused in the back-focal plane but the whole pattern is rotated. The signal and primary electron beams move in the vicinity of the optical axis in opposite directions, so that they can be separated using the Wien filter that directs the signal beam toward a side-attached detector.<sup>6</sup> Two-dimensional image of the specimen can be composed from the four-dimensional data by various methods employing local differences in the diffraction patterns.

In a SLEEM the elastically backscattered electrons strongly dominate the total emission. These electrons preserve their energy during interaction with the specimen and are reaccelerated in the cathode lens back to the primary energy controlled by the high voltage power supply of the electron gun (up to 5 keV in our case). With this energy the electrons also arrive at the detector but their landing energy in the specimen plane ( $10^0$ – $10^1$  eV) is independently adjusted by high voltage bias of the specimen. Hence the energy of the electrons in the electron-bombarded CCD (EBCCD) detector plane can be tailored to achieve a reasonable dynamic range.

The requirements put on the detector can be summarized as follows. The signal electron energy is up to 5 keV and the current is  $10^{-9}$ – $10^{-10}$  A. For the area detector of the angular distribution, the minimum resolution “o by p” is  $8 \times 8$  points, and the resolution of  $64 \times 64$  points is usually sufficient. The minimum dynamic range of the signal electrons is expected to be  $10^3$ , and the maximum time for acquisition of angular distribution at one specimen point is about 2 ms. It

was decided to design the detector on the basis of a low resolution thinned back-side illuminated CCD sensor working in the direct electron-bombarded mode (EBCCD).

### III. ELECTRON-BOMBARDED CCD DETECTOR

For the detector speed, the key parameter of the EBCCD is the electron-bombarded semiconductor (EBS) gain  $G$  (a number of signal electrons in the potential well generated by one incident electron) which is related to the incident particle energy  $E$ . In the case of the real CCD sensor we must calculate the EBS gain  $G$  directly as the ratio of the number of the signal electrons generated in the potential well  $N_w$  to the number of the impinging electrons in the electron beam  $N_b$ :

$$G = \frac{N_w}{N_b} = \frac{E}{3.65 \text{ eV}} \cdot \varepsilon(E), \quad (1)$$

where  $\varepsilon(E)$  is the detection efficiency of the CCD (assuming that the generation of one signal electron in silicon requires 3.65 eV). The number of incident electrons is given by

$$N_b = \frac{I_b T_{\text{int}}}{e}, \quad (2)$$

where  $I_b$  is the current measured by the Faraday cup,  $T_{\text{int}}$  is the integration time, and  $e$  is the charge of the electron. The detection efficiency is defined as the ratio of the detected energy  $E_w$  to the energy incident on the surface of the CCD,  $E_b$ , and it is a function of the incident electron energy  $E$ :<sup>7</sup>

$$\varepsilon(E) = \frac{E_w}{E_b} = \frac{N_w \cdot 3.65 \text{ eV}}{N_b E}. \quad (3)$$

In practice, the front-side illuminated CCD shows a reasonable efficiency ( $\varepsilon > 0.1$ ) at an energy above 8–12 keV, depending on the type of sensor.<sup>7,8</sup> The available thinned back-side illuminated CCDs have an efficiency higher than 0.1 at energies below 5 keV. The dependence of detection efficiency on the incident electron energy is characteristic of the CCD chip, and we cannot change it. For optimum performance it is desirable to match the energy of the signal electron beam to the CCD sensor.

Let us assess the desired parameters from the point of view of the application to SLEEM. Assume the low resolution EBCCD chip with  $64 \times 64$  pixels and the well capacity of  $300 \times 10^3$  electrons, and the signal beam uniformly distributed over the whole detector area. Then the total number of the signal electrons to be generated in all potential wells is  $N_w = 300 \times 10^3 \cdot 64 \times 64 = 1.2 \times 10^9$  electrons. Having the signal beam current  $I_b = 10^{-9}$  A and the integration time  $T_{\text{int}} = 2$  ms, we need the sensor with gain  $G = N_w/N_b = N_w \cdot e/I_b \cdot T_{\text{int}} = 1.2 \times 10^9 \cdot 1.6 \times 10^{-19} / 1 \times 10^{-9} \cdot 2 \times 10^{-3} = 96$  [see Eq. (2)]. From Eq. (1) we get the necessary efficiency as  $\varepsilon(5 \text{ keV}) = 96 \cdot 3.65/5 \times 10^3 = 0.07$ . For  $I_b = 10^{-10}$  A these parameters are  $G = 960$  and  $\varepsilon(5 \text{ keV}) = 0.7$ , respectively.

Let us make another calculation from the point of view of the dynamic range. To achieve a dynamic range of 60 dB we need just 1000 incident electrons to saturate the well (of course with the assumption that dark signal nonuniformity plus noise signal are less than  $300 e^-$ ; this is fulfilled for low integration time even for room working temperature). For a well capacity of the EBCCD chip  $300 \times 10^3 e^-/\text{pixel}$  used we need the chip with  $G = 300$  at the working energy  $E$  of

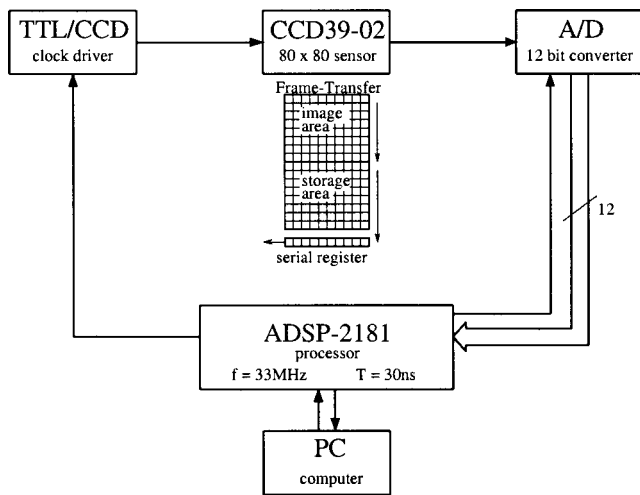


FIG. 2. Electronics of the EBCCD detector.

signal electrons. From Eq. (1) then  $\varepsilon=0.22$  at  $E=5$  keV. Such a more efficient chip would allow us to shorten the integration time or to lower the beam current. Consequently, the thinned back-side illuminated CCD can fulfill our requirements.

The electronics for controlling the CCD sensor and processing the signal data is based on the digital signal processor (DSP) ADSP-2181 (Fig. 2). The DSP generates clock signals to operate the image area, store area, and serial register gates of the frame-transfer operation CCD image sensor and a synchronous clock signal for the 12-bit analog-to-digital (A/D) converter. Clock pulses for CCD are buffered and level shifted by the clock drivers and outputs to the image sensor. The analog output signal from the CCD is synchronously converted pixel by pixel by the 12-bit AD9220 A/D converter, buffered by the line driver to the processor data bus, read, and processed on line. Two voltage levels are sampled and converted for every pixel. The reset level voltage is sampled in the time after reset of the detection node and before the charge transfer to the detection node. The signal level voltage is sampled after the charge transfer. The active video level is obtained by on-line digital subtraction of these two voltages in DSP. In this way, a correlated double sampling is realized.

**IV. EXPERIMENTS AND RESULTS**

The main aim of the experiments and the measurements of the EBCCD sensor was to find an optimum value of energy of the signal electrons. For the first experiment we designed a prototype of the position-sensitive directly bombarded detector of electrons based on the back illuminated high performance CCD sensor CCD39-02 made by Marconi (80×80 pixels—1920 μm by 1920 μm) working in the directly electron-bombardment mode-EBCCD detector. The measurements with the chip bombarded by the electron beam were performed in the low energy SEM developed at our Institute of Scientific Instruments (accelerating voltage 0–5 keV, clean vacuum (chamber 10<sup>-5</sup> Pa, gun 10<sup>-7</sup> Pa), personal computer controlled optical system and specimen stage). A small board with the CCD sensor, amplifier, and

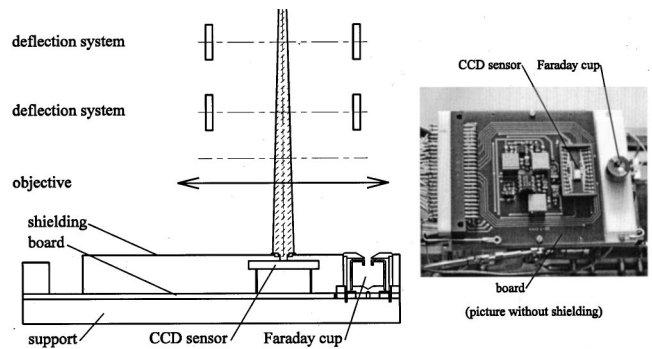


FIG. 3. Experimental setup.

Faraday cup of picoammeter was attached to the  $x$ - $y$  translation stage inside the chamber. The main electronics was situated outside the vacuum. The schematic arrangement of the experimental configuration and the photograph of the board are presented in Fig. 3. The static defocused electron beam was obtained by switching off the objective lens and deflection system. We moved the Faraday cup with a hole of a diameter of 1.6 mm under such an electron beam and measured the beam current  $I_b$ . Next, we moved the shielded CCD sensor with a hole of the same diameter of 1.6 mm under the electron beam and measured the detected output signal  $U_{out}$  as a function of the integration time  $T_{int}$ . The responses for the incident electron energy of 2.5–5 keV are presented in Fig. 4.

**A. Electron-bombarded CCD gain and detection efficiency**

In order to calculate the gain and detection efficiency for certain electron energy  $E$  only one image from the CCD is necessary. From the known current density  $J_b$ , integration time  $T_{int}$ , and output signal of only one pixel of the sensor  $U_{out}$ , we can get  $G$  and  $\varepsilon$ . The saturation of the potential well must be avoided. The problem is that an ideal electron beam with sufficient homogenous current density does not exist in practice. Therefore we cannot calculate the current

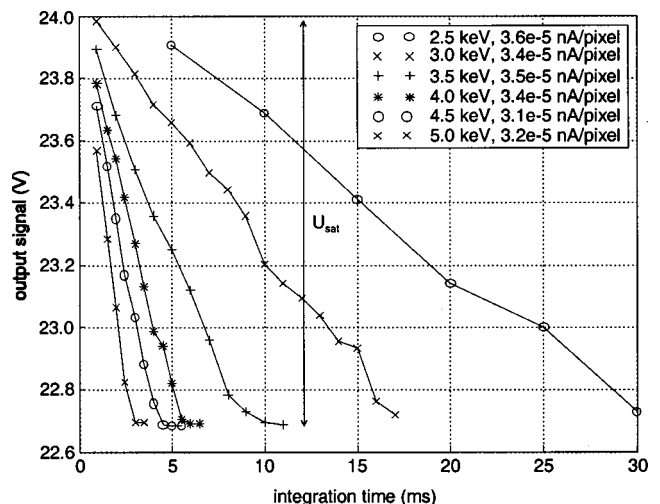


FIG. 4. Output signal  $U_{out}(T_{int})$  for incident electron energy 2.5–5.0 keV (from right to left). The values of the electron current used are presented.

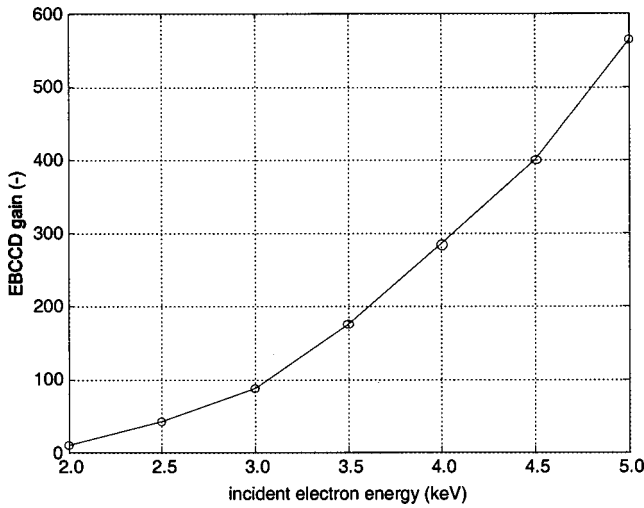


FIG. 5. Electron-bombarded CCD gain.

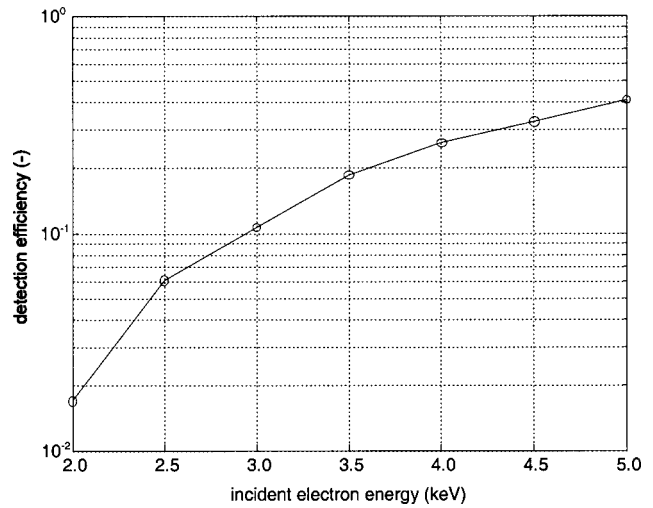


FIG. 6. Electron-bombarded CCD detection efficiency.

impinging on one pixel from the current of the defocused electron beam measured by the Faraday cup. The solution is to use the algorithm based on the definition of the gain extended over all pixels for the calculation: gain is the number of signal electrons in all potential wells over all incident electrons. Such an algorithm makes the calculation of the gain possible even when we use a standard nonhomogeneous electron beam. We have to measure the total electron current  $I_b$  impinging on a certain area of the sensor and the total detected output signal  $U_{out}$  from the same area. This is why we use the same entrance pupils for both the sensor and the Faraday cup. In practice we consider the output signal from the whole image area minus the dark signal generated in all potential wells and suppose that the shielded part of the sensor generates only the dark signal. As a result we get an average gain over all pixels of the sensor.

The number of signal electrons generated in all potential wells  $N_w$  is given by

$$N_w = \frac{\Delta U_{out}}{CCF} = \frac{ADC \cdot AD_{out}}{CCF}, \quad (4)$$

where CCF is the charge conversion factor of the CCD chip,  $AD_{out}$  is the sum of binary video signals over the whole image area of  $80 \times 80$  pixels, ADC is the conversion coefficient between the binary output of A/D converter and the output voltage from the sensor, and  $\Delta U_{out}$  represents the sum of active video signals over the whole image area. The gain

$G$  of the CCD was then calculated from Eq. (1), and the detection efficiency  $\varepsilon$  was calculated from Eq. (3).

For every measured energy  $E$  several CCD images with different integration times were acquired. The current of the defocused beam measured using the Faraday cup was set on an approximately equal level  $\approx 100$  pA for every series of the measurements. This makes possible a comparison of the sensor's sensitivity (i.e., integration time dependence of the output signal) for different energies in one graph (Fig. 4). Because the electron beam cross section was not homogeneous, we chose the data from the most exposed pixel of the image after 2D filtering as an example for Fig. 4. The values of the current impinging on the most exposed pixel are presented in the table included in the graph. The reason for the differences is the noise of the field-emission cathode used. The noise manifests itself on the nonlinear course of the curves. This is why the values of gain and detection efficiency were calculated for every image (i.e., for every  $T_{int}$  measured at the same energy  $E$ ) and afterward averages were calculated, which are shown as the functions of the incident electron energy  $E$  between 2 and 5 keV in Figs. 5 and 6.

**B. Dynamic range and brightness resolution**

The dynamic range  $D$  of the EBCCD for given integration time  $T_{int}$  is limited by the peak output voltage  $U_{sat}$  and by the spurious signals: readout noise  $U_n$ , dark signal  $U_{ds}$ ,

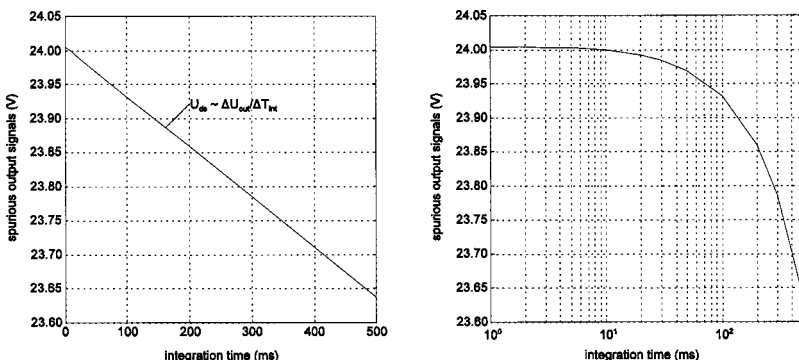


FIG. 7. Average value of the spurious signals over the entire CCD image area.

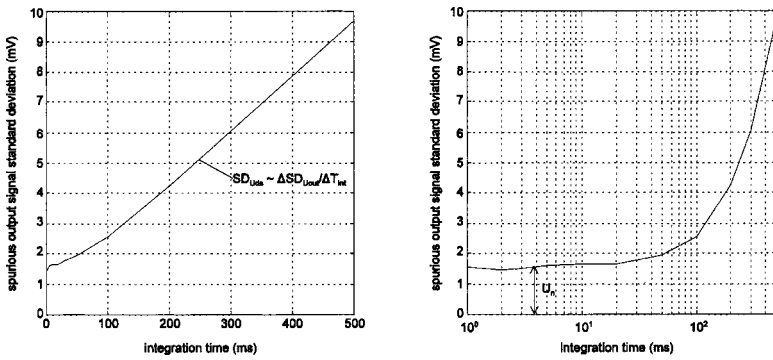


FIG. 8. Standard deviation of the spurious signals over the entire CCD image area.

and dark signal nonuniformity  $SD_{U_{ds}}$ . The peak output voltage  $U_{sat}$  can be obtained from the measurement of the output signal  $U_{out}$  under prolonged bombardment (see Fig. 4). The overall level of the spurious signals can be derived from the measurement of the output signal  $U_{out}$  without illumination (the so-called dark signal) as a function of the integration time  $T_{int}$ . The example of the mean spurious signal is in Fig. 7. The typical time dependence consists of superposition of two components:

- (1) dark signal  $U_{ds}$ —dominant component linear for all pixels so that its nonuniformity  $SD_{U_{ds}}$  can be taken as the standard deviation over the sensor and
- (2) readout noise  $U_n$ —time independent component larger than the dark signal at low integration times.

The dark current can be calculated from the linear part of  $U_{out}(T_{int})$  as

$$I_{ds} = \frac{\Delta q_w}{\Delta T_{int}} = \frac{e \cdot \Delta N_w}{\Delta T_{int}} = \frac{e}{CCF} \cdot \frac{\Delta U_{out}}{\Delta T_{int}} \quad (5)$$

Then the dark current density can be calculated simply as

$$J_{ds} = \frac{I_{ds}}{S_{pixel}} \cdot 10^5 \text{ nA cm}^{-2}, \quad (6)$$

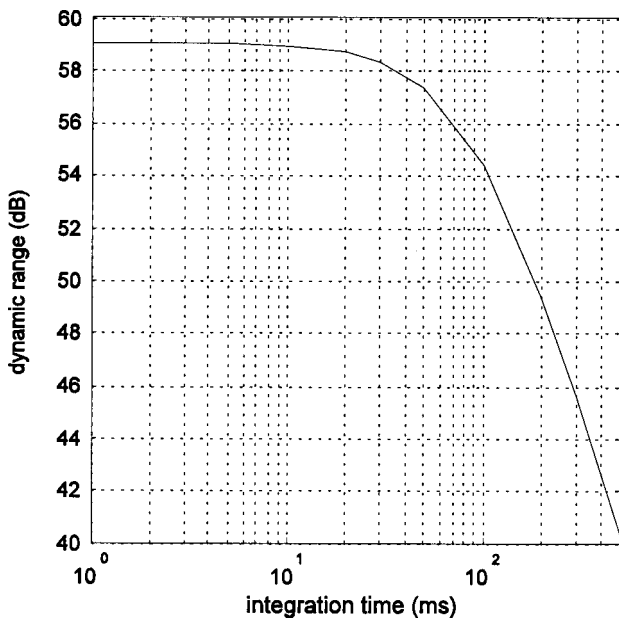


FIG. 9. Dynamic range of the EBCCD detector.

where  $S_{pixel}$  is the pixel area. For the following calculation of the dynamic range it is advantageous to express the dark signal directly as  $U_{ds} = \Delta U_{out} / \Delta T_{int}$  in V/s. The dark signal nonuniformity can be expressed in the same units of V/s.

An example of the standard deviation of the spurious signals over the image area is shown in Fig. 8. The time response has a typical dependence which consist of superposition of two components:

- (1) dark signal nonuniformity  $SD_{U_{ds}}$ —dominant linear component and
- (2) readout noise  $U_n$  (including the noise of all analog circuits between the CCD chip and A/D converter)—time independent component, which can be taken from the nearly constant part of the graph for low integration time; the levels of  $U_n$  and  $SD_{U_{ds}}$  are comparable around the integration time 50 ms when the graph bends upwards.

The dynamic range of the sensor can be calculated as

$$D = 20 \cdot \log \frac{U_{out} - U_{ds} \cdot T_{int}}{\sqrt{U_n^2 + (SD_{U_{ds}} \cdot T_{int})^2}} \quad (7)$$

The values of the dynamic range for integration time up to 500 ms and for room temperature  $\sim 28^\circ\text{C}$  are plotted in Fig. 9. The dynamic range for low integration time, up to 10 ms, is limited mainly by the readout noise. That is why the dynamic range is practically constant for these  $T_{int}$  and reaches  $\sim 59$  dB. At longer  $T_{int}$  the influence of the dark signal and the dark signal nonuniformity starts to prevail.

The brightness resolution  $B$  (the number of the gray levels resolvable in the image) is limited by the CCD well capacity  $N_c$  and EBCCD gain  $G$  and it is given by

$$B = 20 \cdot \log(N_c / G), \quad (8)$$

and its values are listed in Table I.

Now we are ready to assess the optimum energy  $E$  of the signal electrons. For  $B > D$ , i.e., for low electron energies  $E$ , the dynamic range is fully utilized but the number of observ-

TABLE I. Brightness resolution for measured values of the incident electron energy.

$E$ (keV)	2	2.5	3	3.5	4	4.5	5
$G$ (-)	10.9	43.5	89.2	176	284	400	565
$B$ (-)	88.8	76.8	70.5	64.6	60.5	57.5	54.5

able gray levels is limited by the readout noise to  $\sim 59$  dB and the integration time is unnecessarily long. For  $B < D$ , i.e., for high electron energies  $E$ , the brightness resolution is not fully utilized. From the point of view of dynamic range, brightness resolution, and integration time we have an optimum incident electron energy if  $B \approx D$ , which for low integration time is achieved at  $E \approx 4.2$  keV. To achieve  $B \approx D$  we can simultaneously increase  $T_{\text{int}}$  and decrease  $E$  if  $B < D$  or decrease  $T_{\text{int}}$  and increase  $E$  if  $B > D$ .

In practice the integration time strongly depends on the angular distribution of signal electrons that are influenced by the specimen, its surface relief, and at very low energies the crystalline structure. Normally for acquisition of the angular distribution, i.e., the diffraction pattern, with the optimum number of electrons in the potential wells of CCD, only some pixels will be saturated. Therefore the simple case of uniform distribution examined above is the worst case from the point of view of the integration time, while in practice the conditions would be more favorable.

The total dose on the detector during our experiments was approximately  $700 \times 10^6$  electrons/pixel. The radiation damage of the sensor, i.e., an increase in the dark signal generation, amounts to about 9%. The influence of such damage on the dynamic range is still negligible, especially for low integration time.

#### ACKNOWLEDGMENT

The work was supported by the Grant Agency of the Czech Republic under Grant No. 102/00/P001.

<sup>1</sup>E. Bauer, Rep. Prog. Phys. **57**, 895 (1994).

<sup>2</sup>M. Jacka, M. Kirk, M. M. ElGomati, and M. Prutton, Rev. Sci. Instrum. **70**, 2282 (1999).

<sup>3</sup>M. Horáček, J. Comput.-Assist. Microsc. **10**, 23 (1998).

<sup>4</sup>M. Lenc and I. Müllerová, Ultramicroscopy **41**, 411 (1992).

<sup>5</sup>M. Lenc and I. Müllerová, Ultramicroscopy **45**, 159 (1992).

<sup>6</sup>D. Pejchl, I. Müllerová, L. Frank, and V. Kolařík, Czech. J. Phys. **44**, 269 (1994).

<sup>7</sup>D. G. Stearns and J. D. Wiedwald, Rev. Sci. Instrum. **60**, 1095 (1989).

<sup>8</sup>Ch. B. Opal and G. R. Carruthers, Proc. SPIE **1158**, 96 (1989).